Inline high frequency ultrasonic particle sizer

Cite as: Rev. Sci. Instrum. **84**, 075101 (2013); https://doi.org/10.1063/1.4811847
Submitted: 02 May 2013 • Accepted: 11 June 2013 • Published Online: 02 July 2013

F. Lefebvre, J. Petit, G. Nassar, et al.


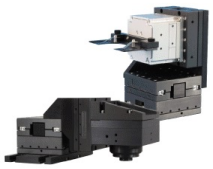
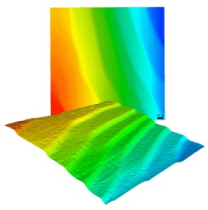
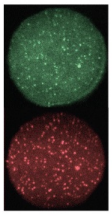

Inline high frequency ultrasonic particle sizer

F. Lefebvre,[1] J. Petit,[2,3] G. Nassar,[1] P. Debreyne,[2] G. Delaplace,[2] and B. Nongaillard[1]
[1]*IEMN, UMR8520 Département d'Opto-Acousto-Electronique, Université de Valenciennes, LeMont Houy, 59313 Valenciennes Cedex, France*
[2]*INRA, UR638 Processus aux Interfaces et Hygiène des Matériaux, 369, rue Jules Guesde BP20039, F-59651 Villeneuve-d'Ascq, France*
[3]*LIBio, Université de Lorraine, 2, avenue de la Forêt de Haye, TSA 40602, F-54518 Vandœuvre-lès-Nancy Cedex, France*

(Received 2 May 2013; accepted 11 June 2013; published online 2 July 2013)

This paper reports the development of a new method of particle sizing in a liquid. This method uses high frequency focused ultrasounds to detect particles crossing the focal zone of an ultrasonic sensor and to determine their size distribution by processing the reflected echoes. The major advantage of this technique compared to optical sizing methods is its ability to measure the size of particles suspended in an opaque liquid without any dedicated sample preparation. Validations of ultrasonic measurements were achieved on suspensions of polymethyl methacrylate beads in a size range extending from a few micrometer to several hundred micrometer with a temporal resolution of 1 s. The inline detection of aggregate formation was also demonstrated. © *2013 AIP Publishing LLC*. [http://dx.doi.org/10.1063/1.4811847]

INTRODUCTION

Food industry, cell engineering, and pharmaceutical manufacturing are some examples of the many fields of engineering research that are facing the problem of particle (e.g., single cell, aggregate, or agglomerate) characterization. Particle characterization is a wide field of study in which many parameters have to be considered: e.g., concentration, size, velocity. Among them, size is probably the most important particle property. However, the notion of particle size should be handled with caution, because size is highly dependent on the analytical method, the considered size estimator, and the particle shape and behavior during analysis. Moreover, most granulometric methods were developed for spherical particles; in consequence, they only measure equivalent spherical diameters of particles, without providing information about their shape.

Apart from optical microscopy combined with image analysis, the most common particle sizing methods are based on light diffraction:[1,2] low angle laser light scattering and quasi-elastic light scattering,[3] the latter also being known as dynamic light scattering. These methods rely on light scattering theories to interpret experimental data.[4] Other methods are based on the individual counting of particles, such as optical extinction counter[1,2] and Coulter counter.[1,5] The major drawback of optical methods is the inability to perform analyses in opaque media. In addition, these methods often require diluting the original suspension, which introduces a bias in the estimation of the size distribution.

Finally, mechanical separation methods,[1] such as fractionation, sedimentation, and centrifugation, are also employed for granulometric purposes. Mechanical methods are invasive and require product sampling. They are not suitable for inline use.

In the last years, ultrasonic methods for particle sizing have emerged. They are grouped under the common designation of ultrasonic spectroscopy.[6,7] When an ultrasonic wave travels a suspension of particles, both wave velocity and attenuation are affected by particle properties (for instance, size distribution) and composition of the surrounding medium. Either employed with continuous waves, tone burst, or broadband pulses, ultrasonic spectroscopy has shown its ability to give access to the particle size distribution by analyzing the frequency dependence of the wave propagation velocity and its attenuation.[6] More recently, the diffraction grating ultrasonic spectroscopy has been developed and this technique shows a great potential in the field of particle characterization.[8] The difficulty inherent to the implementation of ultrasonic methods for particle sizing lies in the need for physical models describing the complex interactions between ultrasonic waves and particles, together with mathematical models enabling the inversion of spectrum data for the calculation of the particle size. In recent years, the modeling of ultrasonic waves propagation in suspensions has experienced a renewed interest, particularly for high-frequency characterization of contrast agents.[9]

The choice of an ultrasonic method for granulometric purposes depends on many factors: nature of the analyzed medium, analytical conditions, size range, analysis rate, and physical properties of particles. On one hand, laboratory applications need high precision instruments that involve complex sample preparation and data processing. On the other hand, in the industrial field of process control, simpler methods should be developed, particularly for inline monitoring applications. Although based on the detection of ultrasonic waves affected by the presence of particles in a fluid, the particle sizing system described in this article is not based on an ultrasonic spectroscopy method. It is based on the detection of individual particles when flowing through a focused ultrasonic beam and permits access to particle size by measuring the number of reflected echoes. The principle of this method was previously established by Lefebvre *et al.*[10–12] when dealing with the feasibility of using high frequency (several

hundreds of megahertz) focused ultrasonic waves to count biological cells. The "Inline High Frequency Ultrasonic Particle Sizer" shares several advantages with common ultrasonic methods, such as no need of a sampling procedure, ability to evaluate particle number and size even in an opaque medium, and no alteration of the medium. This last point is of primary importance in the case of biological samples or for the inline monitoring of food processes.

MATERIAL AND METHODS

Ultrasonic device

The main device of the particle sizing system is the detection chamber shown in Figure 1. The method principle consists in detecting and counting particles flowing through the focal zone of an ultrasonic sensor excited in pulse mode. The particles suspended in a liquid phase are pumped from a tank and injected in the detection chamber. During its circulation through the focal zone, a particle receives ultrasonic pulses each 100 μs and then reflects a part of the ultrasonic energy back to the sensor. Then, the back-scattered pulses are amplified and shaped by a high speed comparator for further interpretation.

The sensor part of the detection chamber is composed of a high frequency ultrasonic sensor working at 350 MHz. This frequency value was a compromise between the desired detection limit for the particle size (around few micrometers) and the attenuation of the ultrasound signal at high frequencies. A lithium niobate ($LiNbO_3$) piezoelectric transducer is bonded at one end of a silica (SiO_2) rod (of 5 mm diameter and 10 mm length). The transducer thickness was adjusted to 10 μm in order to obtain the desired resonant frequency of 350 MHz. A spherical concave lens is machined at the other end of the silica rod. The transducer produces a plane wave ultrasonic beam that propagates and is focused by the lens in the medium in which the sensor is plunged down. The lens has an apparent diameter of 1 mm and an aperture of 60°. The use of such a high aperture without aberration is made possible by the use of silica, which has a high refractive index (n ≈ 4) compared to materials traditionally employed in optics (n ≈ 1.5 for glass). Detection sensitivity is optimized by an adequate choice of the sensor geometry and the working frequency. Indeed, these operating conditions are fixed so as to obtain an ultrasonic focal zone (spot) of comparable or smaller dimensions than the smallest particle size in suspension (micrometric in the case of food particles).[13]

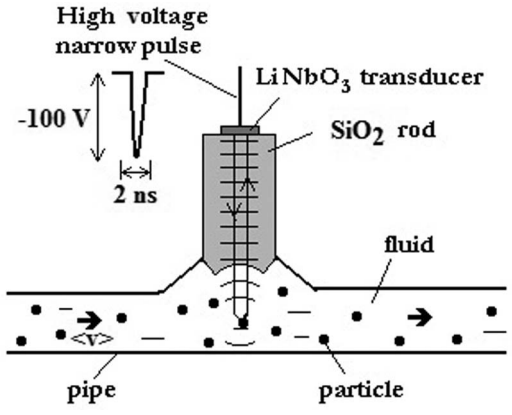

FIG. 1. Ultrasonic device and detection chamber. ⟨v⟩ stands for fluid velocity and arrows inside the pipe indicate flow direction.

Ultrasonic field

In order to adjust the design parameters of the sensor, we developed a numerical code to simulate the ultrasonic field $\Phi(P)$ produced by the sensor. This code is based on the diffraction calculation using Rayleigh-Sommerfeld integrals. Figure 2 shows the geometry of the problem.

The ultrasonic field $\Phi(P)$ is expressed by two nested integrals according to the cylindrical geometry of the problem:

$$\Phi(P) = \int\int_{S'} \left[\int\int_{S} \Phi_0 \frac{e^{j\vec{k}.\vec{r}}}{\|\vec{r}\|} dS \right] \cdot T(\theta) \frac{e^{j\vec{k}'\vec{r}'}}{\|\vec{r}'\|} dS', \qquad (1)$$

where S and S′ are, respectively, the surfaces of the transducer and the lens. Vector $\vec{r}$ points from an infinitesimal point source of S to a point located on the lens S′. Vector $\overrightarrow{r'}$ points from this later point to the observation point P located in the medium. $\vec{k}$ and $\overrightarrow{k'}$ are, respectively, the wave vectors in the buffer rod and in the medium.

The integral in brackets describes the radiation of the transducer, as evaluated at a point belonging to the surface of the spherical lens inside the buffer rod. The vibration of the transducer surface S is represented by the potential function Φ_0, which can be considered as uniform close to the surface of the transducer. T(θ) is the dimensionless angular transmission coefficient of the lens at the silica-fluid interface. The outer integral over S′ stands for the lens radiation in the investigated medium.

Numerical calculations have been carried out around the focal zone (20λ before and 10λ after the focal zone, where λ is the wavelength in the propagation medium) that would be obtained with the optical approximation, i.e., for a focal length $f_{opt} = \frac{nR}{n-1}$ where R is the curvature radius of the lens and n the refractive index.

Focus depth and diameter obtained by simulation using the optics approximation were compared to the

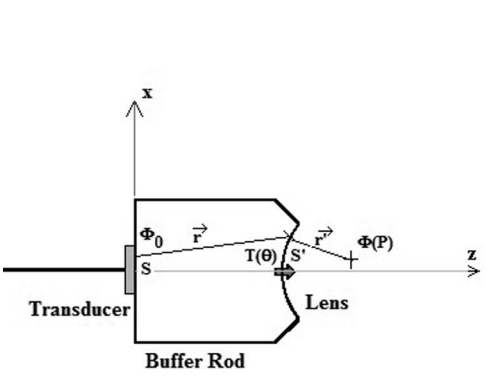

FIG. 2. Ultrasonic device geometry, as considered in the calculation of the ultrasonic field.

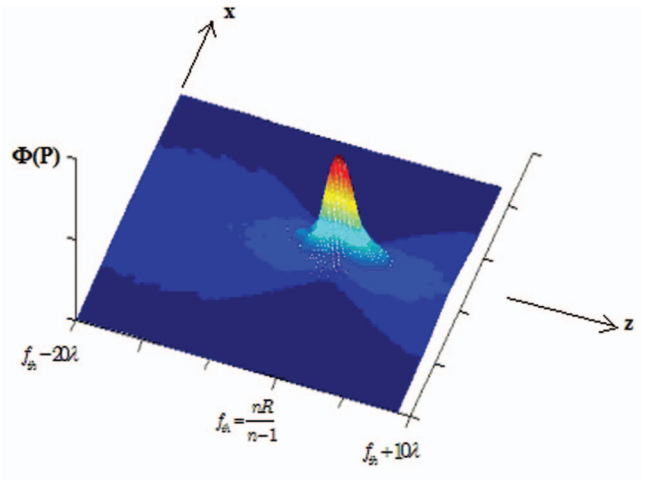

FIG. 3. Simulation of the ultrasonic spot produced by the 1 mm/±30° focused sensor at 350 MHz.

experimental recordings of the ultrasonic field. The calculations were performed by considering water as the propagation medium. Figure 3 shows the ultrasonic field map obtained by simulation of the Rayleigh-Sommerfeld integral. A very sharp ultrasonic spot was obtained, which indicates that the ultrasonic energy is concentrated in a small volume, corresponding to the detection volume. Figure 4(a) shows the −3, −6, and −20 dB contours of the spot. The geometrical parameters of the focal zone were measured on the basis of the −3 dB contour. A focal distance of 1040 μm and a focal depth of 48 μm were predicted from this simulation. Figure 4(b) shows the section of the field in the focal plane (Ox). This permitted to evaluate a focal zone diameter of 6.2 μm. When analyzing particles suspended in water at 20 °C, the wavelength of the ultrasonic waves at 350 MHz was estimated at about 4.3 μm. With a large lens aperture, it is common to observe a focal zone diameter around 2λ and a focal depth around 10λ.[14] The simulations provided consistent values with these considerations.

Figure 5 shows the experimental recording of the acoustic field produced by the sensor in the direction (Ox). This measurement was obtained by moving the probe alongside a razor blade in the focal plane.[10,11] The level of the reflected echo was recorded, smoothed, and derived in order to obtain the field distribution in the focal plane. The value of the −3 dB focus diameter was obtained (7.2 μm) with a good agreement with simulations. The focal depth could be estimated by the V(z) method[13] on a target that does not allow the generation of the Rayleigh wave in water. This overcomes the problem of the ultrasonic signature of the target (lead). A focal depth of 50 μm and a focal distance of 1044 μm were measured. Table I illustrates the consistency between simulated and experimental values of focus width, field depth, and focal distance.

TABLE I. Simulated and experimental ultrasonic field characteristics.

(μm)	Simulation	Expt.
Focus width W	6.2	7.2
Field depth P	48	50
Focal distance f	1040	1044

Principle of ultrasonic granulometry

The particle flux φ_t (s^{-1}) crossing the focal zone is related to the number of particle per unit volume n (m^{-3}) and mean flow velocity $\langle v \rangle$ ($m\,s^{-1}$) according to Eq. (2):[10]

$$\varphi_t = K n \langle v \rangle, \tag{2}$$

where K (m^2) is function of the surface crossed by particles during their flow. Actually, this surface, also called "detection surface," is the outer surface of the focal zone. It is reasonable to consider that the spot has approximately an ovoid shape according to the −3 dB contour Fig. 4(a).

A particle with a mean velocity $\langle v \rangle$ will take a defined time to cross the ultrasonic spot, called the particle transit time t_t in this paper. It corresponds to the time during which the particle is detected by the sensor. If the transit time is greater than the recurrence rate T_r of ultrasound pulses, the same particle intercepts several consecutive ultrasonic shots and generates a set of reflected echoes. At a constant flow velocity $\langle v \rangle$, the transit time is proportional to the particle diameter d, as indicated in Eq. (3):

$$t_t = \gamma \mathrm{d}. \tag{3}$$

The coefficient γ ($s\,m^{-1}$) depends on the size of the ultrasonic spot, on the threshold used to trigger the detection, and on the particle velocity. Figure 6 depicts this phenomenon in the particular case where a particle produces three reflections.

The flow velocity was chosen sufficiently low (less than 1 cm s^{-1}) so that the condition $t_t < T_r$ was practically always verified. Practically, particles with diameter as small as 2 μm can be detected with $T_r = 100\,\mu$s. As the suspending medium is diluted, bursts of reflected echoes corresponding to the presence of a particle in the spot are separated by "silences" corresponding to ultrasound shots without particle. The echographic signal, displayed in Figure 7, is therefore composed of bursts of pulses repeated at T_r rate separated by silences.

By counting over a given period the number of reflected pulses N_t as well as the number of burst or "pulse packets" N_p, we can calculate the average number of reflected pulses on a particle per burst $\langle N_{tp} \rangle$, which is related to the ratio between the transit time t_t and the recurrence rate T_r (and therefore to the particle diameter d), as expressed in Eq. (4):

$$\langle N_{tp} \rangle = \left\langle \frac{N_t}{N_p} \right\rangle = \frac{t_t}{T_r} = \frac{\gamma d}{T_r}. \tag{4}$$

The average number of echoes per burst $\langle N_{tp} \rangle$ over a given period provides an indicator of the mean size of particles that crossed the ultrasonic spot during this period. By repeating the process continuously, this system is able to build the particle size distribution.

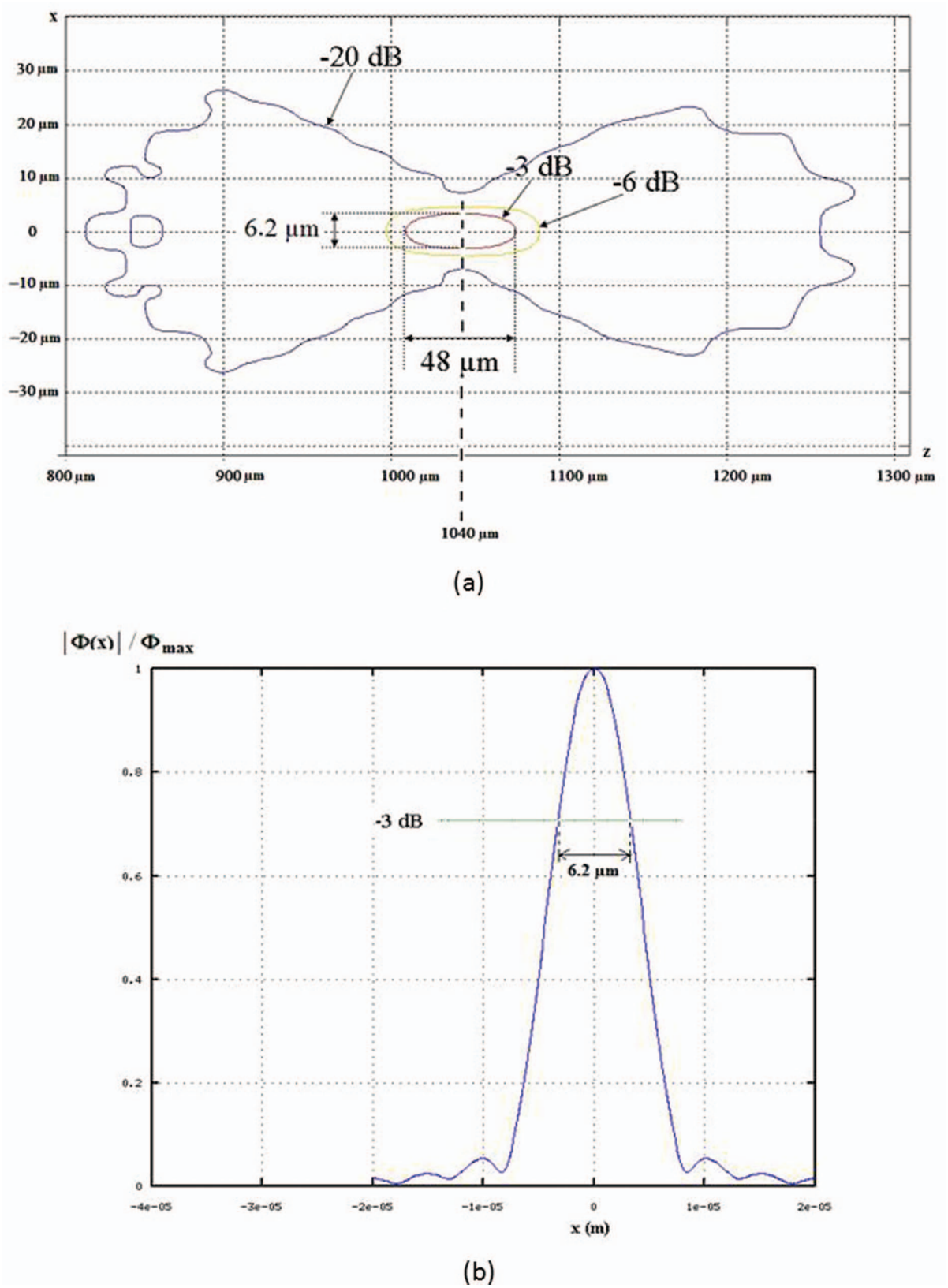

FIG. 4. (a) Contour plot of the ultrasonic spot at −3, −6, and −20 dB. (b) Simulated field profile in the focal plane (at 1040 μm from the lens).

Overview of the system

The experimental setup developed in this study is displayed in Figure 8(a). The analyzed fluid is pumped to the ultrasonic transducer emitter by derivation, which permits the inline implementation of the ultrasonic device directly on the pipe of an industrial process.

The ultrasonic sensor is excited by ultra-short (≅2 ns) high-voltage pulses (≅100 V). Pulses are repeated each

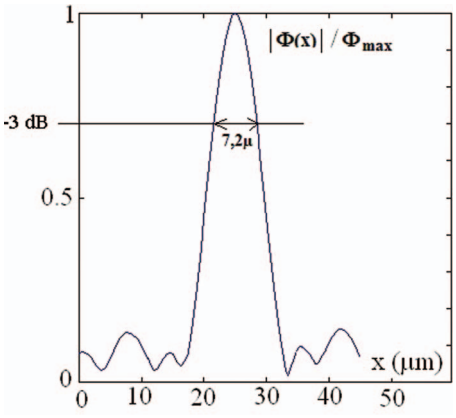

FIG. 5. Experimental field profile (normalized amplitude).

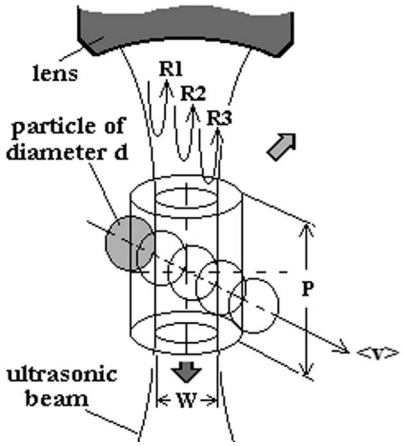

FIG. 6. Multiple echoes from a single particle crossing the ultrasonic spot at constant speed $\langle v \rangle$.

100 μs. The reflected signal is routed through a broadband directional coupler to a 30 dB wide band amplifier. A time window allows to select specifically the part of the ultrasonic signal corresponding to the acoustic spot. An ultra-fast comparator (aperture time of 0.5 ns) is used to detect a reflected echo directly in the high frequency signal. Figure 8(b) shows a typical high frequency echo (A) reflected from a particle and its corresponding shaped pulse in TTL compatible format (B). A small time shift due to the propagation delay in electronic components can be observed.

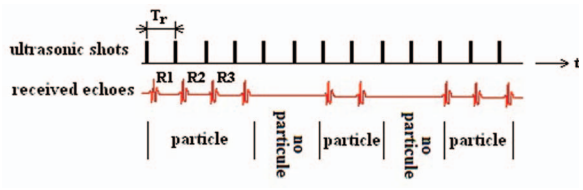

FIG. 7. Example of an echographic signal.

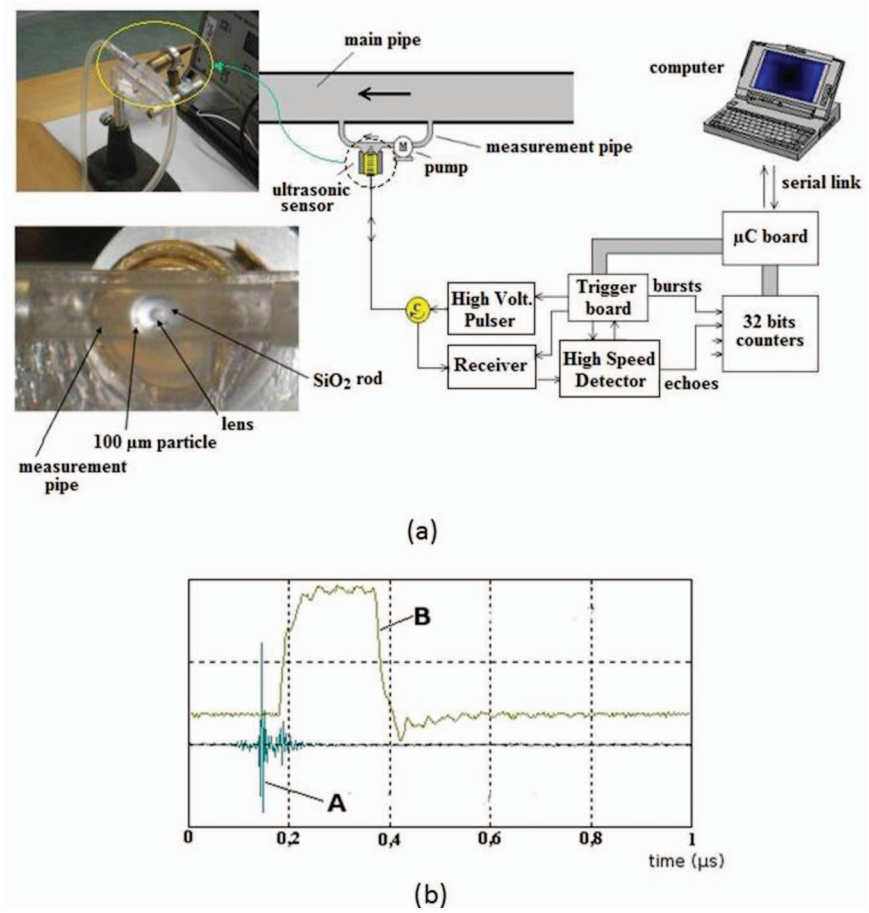

FIG. 8. (a) Overview of the inline high frequency ultrasonic particle sizer. (b) A typical echo reflected by a particle (A) and its shaped pulse (B).

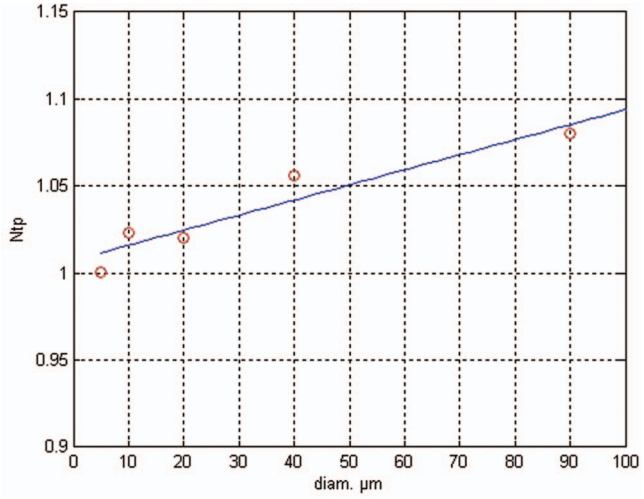

FIG. 9. Calibration of the system. Average number of pulses per burst versus diameter of standard particles in μm.

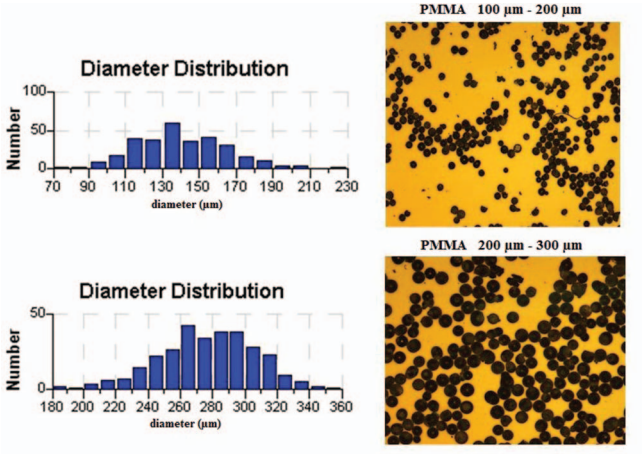

FIG. 10. Optical microscope size analysis of two samples of PMMA spheres.

A trigger board allows to drive synchronously the transmitter and receiver, as well as to elaborate the burst signal corresponding to the particle flowing through the ultrasonic spot. Reflected echoes and their corresponding bursts are counted during a specified time with 32-bit counters. The whole system is managed by a microcontroller board that also drives a serial link with a portable computer.

RESULTS

The system was calibrated with standards of monodispersed PMMA spheres. Five diameters were used: 5, 10, 20, 40, and 90 μm. For each sample, reflected pulses and bursts were counted during 30 s and the number of pulses per burst N_{tp} was calculated. The protocol was repeated during 2 h to provide 240 values of N_{tp}. For each particle size, the statistical distribution of N_{tp} was built and the average value $\langle N_{tp} \rangle$ was determined over 30 s and correlated with the particle size provided by the manufacturer. The average value of $\langle N_{tp} \rangle$ versus particle diameter is shown in Figure 9. A very good linear correlation ($R^2 = 0.93$) between $\langle N_{tp} \rangle$ and the diameter of the standard particles was observed, indicating the validity of Eq. (4).

Tests were then conducted with two mixed PMMA samples. These samples were prepared by sieving (Retsch sieves), one between 100 and 200 μm and the other between 200 and 300 μm. For both samples, a particle sizing was carried out by

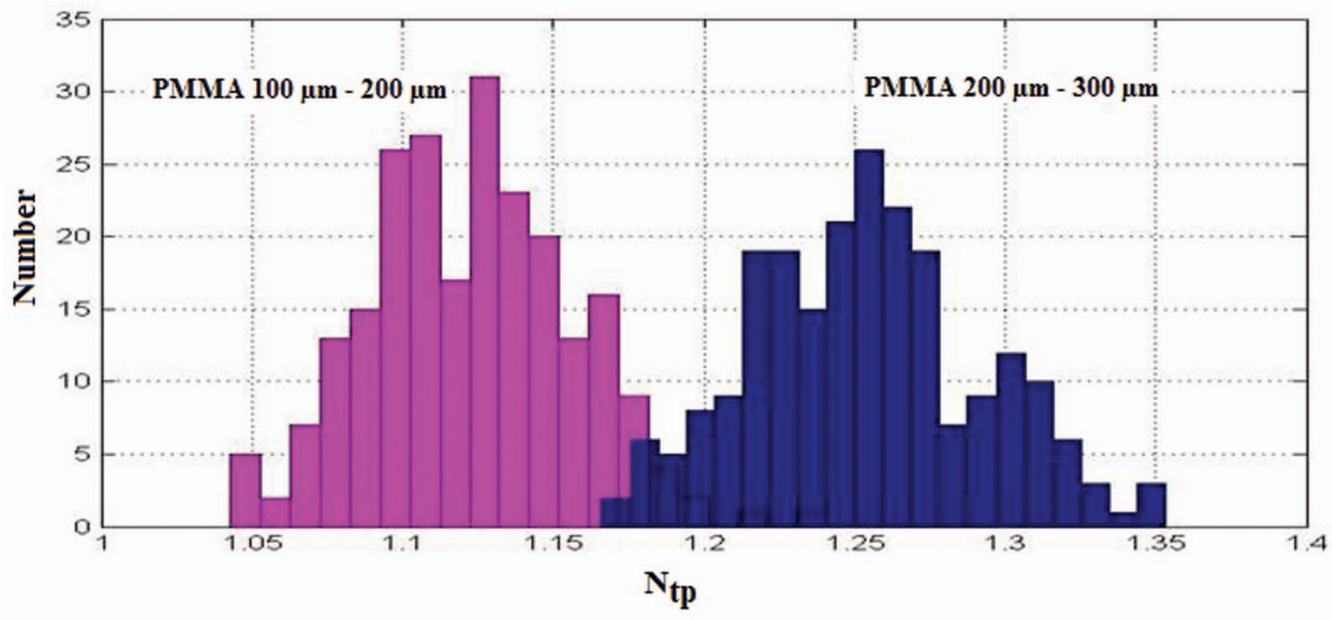

FIG. 11. Ultrasonic N_{tp} distribution law for the 100–200 μm and 200–300 μm PMMA mixed samples.

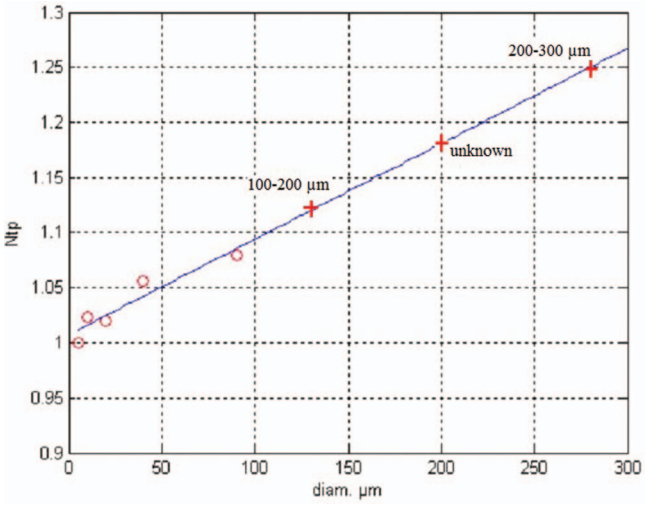

FIG. 12. Correlation between optical and ultrasonic measurements according to the calibration curve.

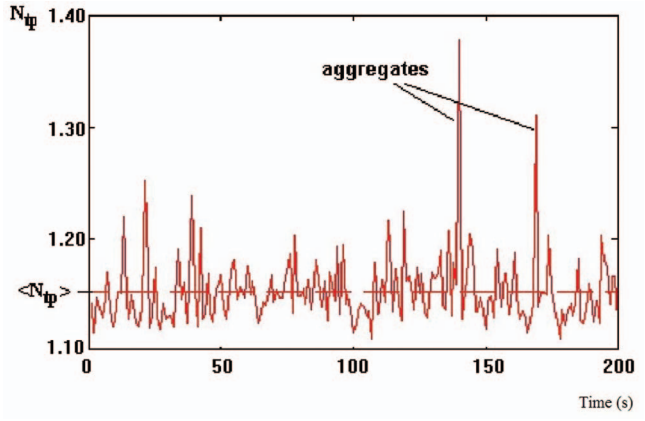

FIG. 14. Temporal evolution of N_{tp} in the presence of aggregates in the suspension.

optical means using a microscope (Nikon AZ100) equipped with a camera (Nikon DS-Ri1) combined with an image analysis software (Nikon NIS Elements). Figure 10 shows the size distribution of the two samples obtained by microscopic measurements. The simple sieving method led to relatively broad size distributions.

The numbers of pulses per burst N_{tp} were measured in the same experimental conditions as for standards. Histograms of N_{tp} distributions were plotted in Figure 11. The corresponding average values $\langle N_{tp} \rangle$ were calculated and plotted on the calibration curve (Figure 12). This permitted to highlight that the linear correlation between N_{tp} and particle diameter, established in Figure 9, remained valid for these mixed samples, even if their size was outside the calibration range.

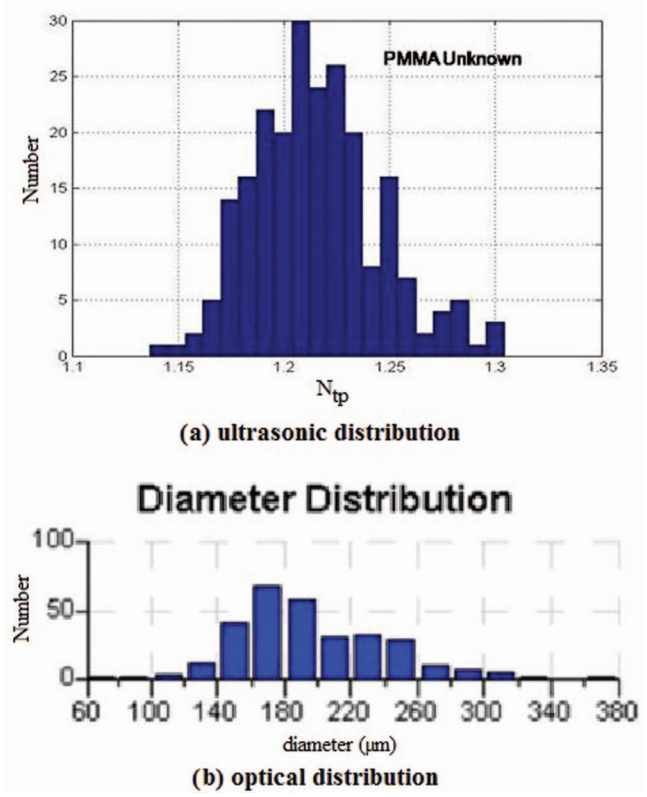

FIG. 13. Ultrasonic (a) and optical distributions (b) for the unknown sample.

To check the validity of the ultrasonic particle size measurement, a third sample was analyzed with our ultrasonic device. This sample is referred as "unknown" because it has been prepared under non-controlled sieving conditions. After recording N_{tp}, the average diameter of the particles was estimated from the calibration curve (Figure 12). This mean diameter was confirmed by optical microscope analysis. Figure 13 shows the ultrasonic (a) and optical (b) distributions of N_{tp}.

In some experiments, we observed the formation of particle clusters (formed by electrostatic effect due to friction during flowing). The formation of clusters in the suspensions was notable from the temporal record of N_{tp}. This record may exhibit peaks of abnormally high values compared to the mean value. An example of record is shown in Figure 14.

By continuously plotting the distribution of N_{tp}, we observed the emergence of modes of higher mean values than the major trend. Small clusters give values of N_{tp} close to the predominant mode, having a distortion effect on the major trend, while larger values produce modes that are clearly distinguishable from the predominant mode. Figure 15 shows the changes in the distribution of N_{tp} owing to the aggregation of PMMA spheres during analysis. Currently, the experimental size distribution is fitted with a theoretical mixture of Gaussian distributions using a maximum likelihood technique. Each value of $\langle N_{tp} \rangle$ corresponding to the predominant mode and the abnormal modes is extracted and the corresponding size is computed from the calibration curve (Fig. 12). This method provides an average aggregate size with a precision that varies inversely with the asymmetry of aggregates.

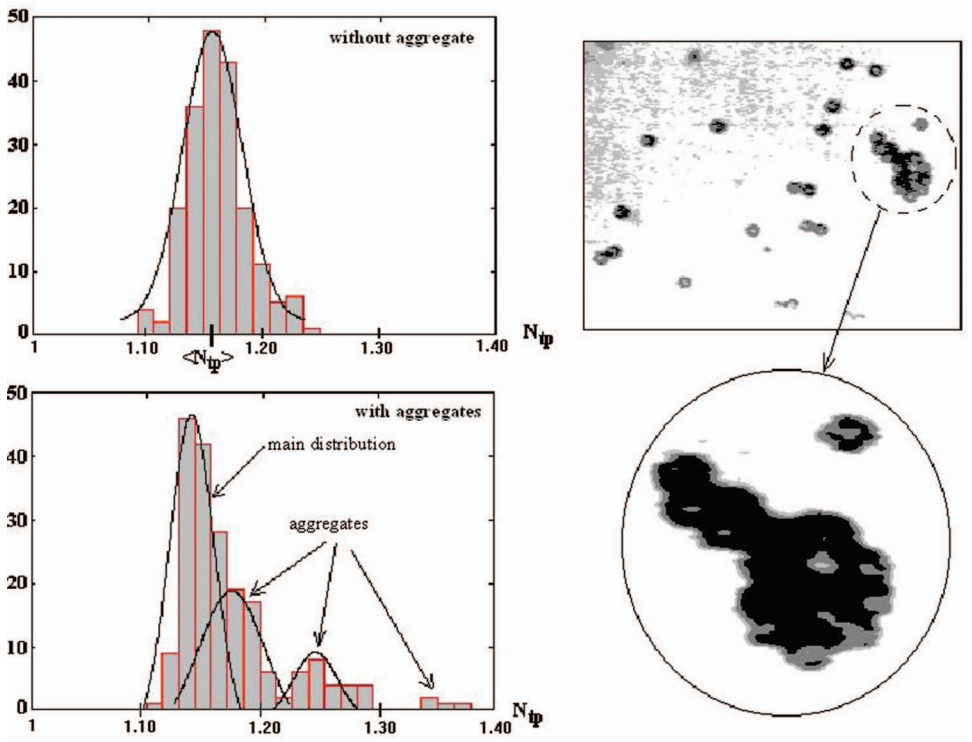

FIG. 15. Changes in the N_{tp} distribution due to the presence of aggregates.

CONCLUSION

In this paper, a new method of particle sizing based on the detection of single particles by the use of high-frequency focused ultrasounds was presented. This method is derived from a particle counting technique previously developed by the authors. The use of ultrasounds allows the investigation of optically opaque media and does not require any sample preparation. In the current state, this method is not as accurate as conventional methods of particle sizing such as laser diffraction granulometry. However, it is an effective way to monitor particle size requiring no transparency of the suspension and being adapted to inline characterization. Technological improvements need to be made to achieve a level of accuracy comparable to conventional methods. A simple model of particle size measurement was validated by the strong linear correlation between the number of reflected echoes per burst and the particle size. This ultrasound granulometer showed its ability to detect the apparition of aggregates and follow their size evolution. Many applications can be envisaged for this inline high frequency ultrasonic particle sizer, especially in the food industry where the fine characterization of particle size is required, as it influences several important product functionalities (such as organoleptic and handling properties).

ACKNOWLEDGMENTS

This work constituted a part of the sensor development workpackage of the Globule project ANR-08-ALIA-08. The authors wish to thank the French National Research Agency for financial support.

[1]T. Allen, *Particle Size Measurement*. Powder Technology Series, 5th ed. (Chapman Hall, 1996).
[2]R. Xu, *Particle Characterization: Light Scattering Methods*. Particle Technology Series Vol. 13 (Kluwer Academic Publishers, 2000).
[3]W. Tscharnuter, *Photon Correlation Spectroscopy in Particle Sizing*, Encyclopedia of Analytical Chemistry, edited by R. A. Meyers (John Wiley & Sons Ltd, 2006).
[4]T. Wriedt, "A review of electric light scattering theories," Part. Part. Syst. Charact. **15**, 67–74 (1998).
[5]Coulter Electronics, *Coulter Counter and Other Coulter Scientific Instruments: Industrial Bibliography* (Coulter Electronics, 1992).
[6]D. J. McClements, *Ultrasonic Measurements in Particle Size Analysis*. Encyclopedia of Analytical Chemistry, edited by Robert A. Meyers (John Wiley & Sons Ltd, Chichester, 2006).
[7]R. E. Challis, M. J. W. Povey, M. L. Mather, and A. K. Holmes, "Ultrasound techniques for characterizing colloidal dispersions," Rep. Prog. Phys. **68**, 1541–1637 (2005).
[8]M. S. Greenwood and S. Ahmed, "Ultrasonic diffraction grating spectroscopy and characterization of fluids and slurries," Ultrasonics **44**, e1384–e1393 (2006).
[9]F. Coulouvrat, J. L. Thomas, K. Astafyeva, N. Taulier, J. M. Conoir, and W. Urbach, "A model for ultrasound absorption and dispersion in dilute suspensions of nanometric contrast agent," J. Acoust. Soc. Am **132**(6), 3748–3759 (2012).
[10]F. Lefebvre, "Comptage de particules par ultrasons haute fréquence focalisés. Application au génie biologique et médical," Ph.D. Thesis, University of Valenciennes, 1993.
[11]F. Lefebvre, M. Toubal, E. Radziszewski, Y. Deblock, and B. Nongaillard, "Counting biological cells with high frequency focused ultrasounds," *Ultrasonic Imaging* (Plenum Press, New York, 1993), Vol. 20.
[12]F. Lefebvre, M. Ouaftouh, B. Nongaillard, and E. Radziszewski, "Détection de particules biologiques en suspension par ultrasons haute fréquence," J. Phys. IV France **4**, C5-1259–C5-1262 (1994).
[13]J. Petit, A.-L. Herbig, A. Moreau, J.-F. Le Page, T. Six, and G. Delaplace, "Granulomorphometry: a suitable tool for identifying hydrophobic and disulfide bonds in β-lactoglobulin aggregates. Application to the study of the aggregation mechanisms occurring in a β-lactoglobulin concentrate between 70 and 95 °C," J. Dairy Sci. **95**, 4188–4202 (2012).
[14]G. A. D. Briggs and O. V. Kolosov, *Acoustic Microscopy*, 2nd ed. (Oxford University Press, 2010).